

# PROCEEDINGS OF SPIE

[SPIDigitalLibrary.org/conference-proceedings-of-spie](https://spiedigitallibrary.org/conference-proceedings-of-spie)

## Multi-level analysis of spatio-temporal features in non-mass enhancing breast tumors

Tahmassebi, Amirhessam, Ngo, Dat, Garcia, Antonio, Castillo, Encarnacin, Morales, Diego, et al.

Amirhessam Tahmassebi, Dat Ngo, Antonio Garcia, Encarnacin Castillo, Diego P. Morales, Katja Pinker-Domenig, Mark Lobbes, Anke Meyer-Bäse, "Multi-level analysis of spatio-temporal features in non-mass enhancing breast tumors," Proc. SPIE 10662, Smart Biomedical and Physiological Sensor Technology XV, 106620H (14 May 2018); doi: 10.1117/12.2304928

**SPIE.**

Event: SPIE Commercial + Scientific Sensing and Imaging, 2018, Orlando, Florida, United States

# Multi-level analysis of spatio-temporal features in non-mass enhancing breast tumors

Amirhessam Tahmassebi<sup>a,\*</sup>, Dat Ngo<sup>a</sup>, Antonio Garcia<sup>b</sup>, Encarnacin Castillo<sup>b</sup>, Diego P. Morales<sup>b</sup>, Katja Pinker-Domenig<sup>a,c,d</sup>, Mark Lobbes<sup>e,f</sup>, and Anke Meyer-Bäse<sup>a</sup>

<sup>a</sup>Department of Scientific Computing, Florida State University, Tallahassee, Florida, USA

<sup>b</sup>Department of Electronics and Computer Technology, University of Granada, Spain

<sup>c</sup>Department of Radiology, Breast Imaging Service, Memorial Sloan Kettering Cancer Center, New York, USA

<sup>d</sup>Department of Biomedical Imaging and Image-Guided Therapy, Division of Molecular and Gender Imaging, Medical University of Vienna, Vienna, Austria

<sup>e</sup>Department of Radiology, Maastricht Medical Center, University of Maastricht, Netherlands

<sup>f</sup>GROW School for Oncology and Developmental Biology, Maastricht, Netherlands

## ABSTRACT

Diagnostically challenging breast tumors and Non-Mass-Enhancing (NME) lesions are often characterized by spatial and temporal heterogeneity, thus difficult to detect and classify. Differently from mass enhancing tumors they have an atypical temporal enhancement behavior that does not enable a straight-forward lesion classification into benign or malignant. The poorly defined margins do not support a concise shape description thus impacting morphological characterizations. A multi-level analysis strategy capturing the features of Non-Mass-Like-Enhancing (NMLEs) is shown to be superior to other methods relying only on morphological and kinetic information. In addition to this, the NMLE features such as NMLE distribution types and NMLE enhancement pattern, can be employed in radiomics analysis to make robust models in the early prediction of the response to neo-adjuvant chemotherapy in breast cancer. Therefore, this could predict treatment response early in therapy to identify women who do not benefit from cytotoxic therapy.

**Keywords:** Non-Mass-Enhancing Lesions, Neo-Adjuvant Chemotherapy, Classification, Computer-Aided Diagnosis, Breast Magnetic Resonance Imaging

## 1. INTRODUCTION

Non-mass enhancing (NME) lesions on dynamic contrast-enhanced Magnetic Resonance Imaging (DCE-MRI) are challenging for both radiological assessment and current computer-aided diagnosis (CAD) systems. NMEs are neither well defined in morphology, i.e. geometric shape, nor kinetics, i.e. temporal enhancement, and thus pose a considerable challenge for lesion detection and classification. Although, their phenotypic appearances and differences can be visualized by DCE-MRI, the diagnosis of NME lesions remains challenging.

It was shown in different articles that shape descriptors cannot capture the lesions due to an atypical kinetic behavior for malignant and benign lesions, and also due to poorly defined borders<sup>1-5</sup>. However, non-invasive ductal carcinomas in situ, lobular carcinoma in situ, atypical ductal hyperplasia, papillomas, and benign lesions are such non-mass-enhancing lesions that are easily overlooked and may require a second reading. CAD systems are specialized for automated detection and diagnosis of mass-enhancing lesions that are well characterized by shape and kinetics descriptors according to the BI-RADS lexicon. To overcome these problems and revolutionize the state-of-the-art CAD in breast MRI, we need to focus on correctly capturing and analyzing the unique spatio-temporal behavior of non-mass-enhancing lesions.

---

\* Corresponding Author: Amirhessam Tahmassebi

E-mail: atahmassebi@fsu.edu

URL: www.amirhessam.com

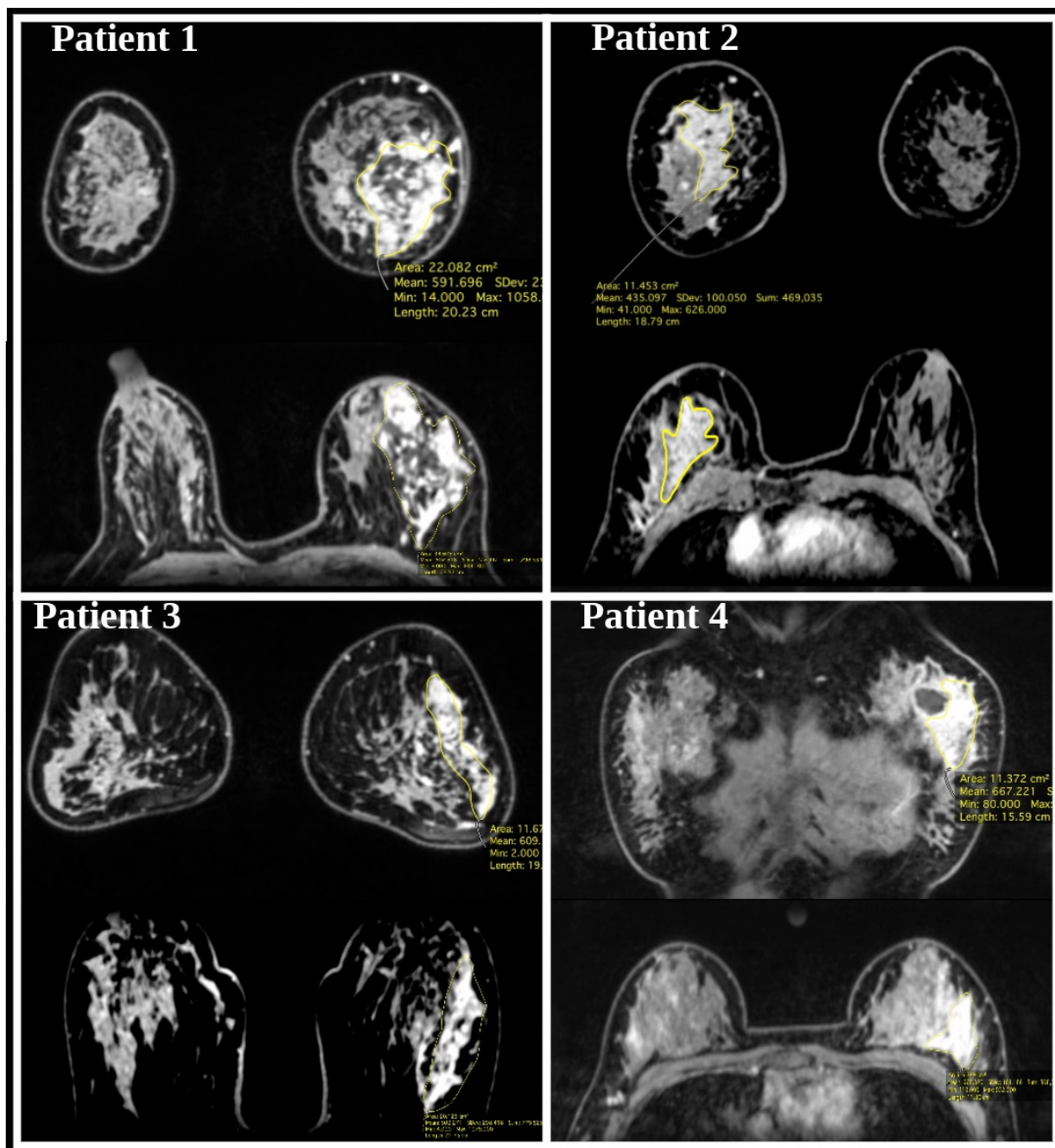


Figure 1. Breast scans of four patients at baseline NAC. NMEs are annotated with yellow line.

Our hypothesis is that a multi-level analysis of features extracted from NMEs based on a concatenation of voxel-wise kinetic feature mapping, spatial association features, and kinetic association features can capture phenotypic subtleties of tumors better than a single feature class.<sup>6-9</sup>

We propose to apply a multi-level analysis strategy to enhance the discriminating power of spatio-temporal association features for an improved prediction of tumor malignancy with DCE-MRI which will improve the

utility of the CAD systems quantitatively.

In addition to this, we investigate the importance of NME features in radiomics using multi-parametric features in early prediction of response to neo-adjuvant chemotherapy employing DCE-MRI at baseline. Neo-adjuvant chemotherapy (NAC) is the treatment of choice in patients with locally advanced breast cancer to reduce tumor burden and potentially enable breast conservation. Early identification of non-responders is crucial as these patients might require different, or more aggressive, treatment to reach a pathological complete response (pCR), or a minimal residual disease which is associated with an improved overall survival.<sup>10-12</sup>

In this paper, novel techniques for establishing the automated diagnosis of NME lesions, and also their connection with NAC were presented and thus improved the quality of breast MRI post-processing, reduced the number of missed or misinterpreted cases leading to false-negative diagnoses.

## 2. MATERIALS AND METHODS

### 2.1 Patients

The database for NME lesions includes a total of 46 patients images, all female. All patients had histopathologically confirmed diagnosis from image-guided breast biopsy and surgical removal. Histologic findings were malignant in 24 and benign in 22 lesions.

### 2.2 MR Imaging

MRIs were performed with a 1.5 T system (Magnetom Vision, Siemens, Erlangen, Germany) equipped with a dedicated surface coil to enable simultaneous imaging of both breasts for both types of lesions. The patients were placed in a prone position for the MRI.

Transversal images were acquired with a STIR (short TI inversion recovery) sequence (TR=5600 ms, TE=60 ms, FA=90°, IT=150 ms, matrix size 228×182 pixels, slice thickness 3 mm). Subsequently, a dynamic T1-weighted gradient echo sequence (3D fast low angle shot sequence) was performed (TR=4.9 ms, TE=1.83 ms, FA=12°) in transversal slice orientation with a matrix size of 352×352 pixels and an effective slice thickness of 1 mm. The dynamic study consisted of 5 measurements with an interval of 1.4 minutes. The first frame was acquired before injection of paramagnetic contrast agent (gadopentatate dimeglumine, 0.1 mmol/kg body weight, Magnevist<sup>TM</sup>, Schering, Berlin, Germany) immediately followed by the 4 other measurements.

In addition to this, 4 patients with biopsy-proven breast cancer scheduled for neo-adjuvant chemotherapy, were included and underwent multi-parametric MRI with T2-weighted, DCE-MRI, and DWI study. Breast MRIs were performed prior to and after two cycles of NAC, and pCR was assessed after surgery. All the T1-weighted DCE-MRI (TR=3.62 ms, TE=1.4 ms, matrix size 192×192 pixels, slice thickness 1.7 mm isotropic, with 72 slices) were taken using a 3.0 Tesla MRI unit (Trio Tim; Siemens Medical Solutions, Erlangen, Germany) with a dedicated four-channel breast coil (In Vivo, Orlando, FL, USA) with. Figure 1 shows the breast scans of patients at baseline NAC. NMEs are annotated in yellow.

## 3. MULTI-LEVEL FEATURE EXTRACTION AND CLASSIFICATION

### 3.1 Lesion Segmentation

Tumor segmentation represents the correct identification of the spatial location of a tumor. Manual segmentation performed by a radiologist is considered the gold standard. However, expert segmentation is not highly precise, prone to inter-observer and intra-observer variability and it might include non-enhancing tissue. It is time consuming viewing both spatial and temporal profiles and thus examining many series of enhanced data and profiles of pixels to determine the lesion boundary. To overcome these problems we employ as an automatic segmentation method an active contour segmentation without edges as proposed by Chan and Vese.<sup>13</sup> Using this method we can detect the interior contours automatically and we can put the initial contour anywhere in the image. Moreover, it is robust with respect to the noise. Other methods for lesion segmentation are based on independent component analysis (ICA) techniques.<sup>14-16</sup>

A precise lesion segmentation method must operate at the same time in the feature (enhancement) space as well as in the image space such that a spatially coherent segmentation is obtained without any subsequent post-processing. Therefore, we enhance the above contour model such that its boundaries are attracted to locations of high confidence. This is achieved by introducing an additional term (external force) that controls the contour evolution. There are hardware tools that can speed up this computation including GPU machines.<sup>17-21</sup>

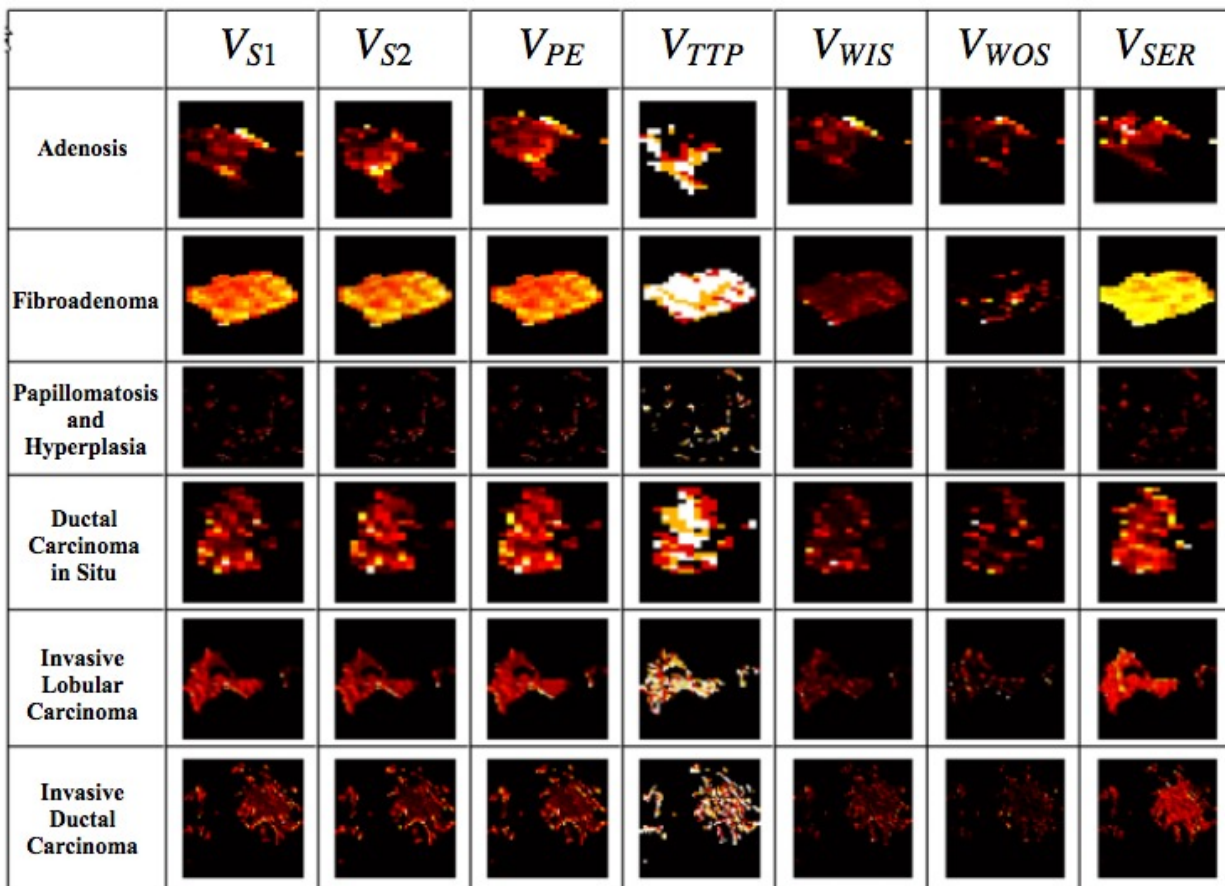


Figure 2. Kinetic feature maps for typical malignant and benign non-mass-enhancing lesions. These maps shows the early post-contrast, late post-contrast, peak enhancement, time-to-peak, wash-in-slope, wash-out-slope and the signal-enhancement ratio. The first three rows are typical benign lesions while the last three rows are malignant non-mass-enhancing lesions.

### 3.2 Feature Extraction

At the first step, a number of voxel-wise kinetic feature maps are calculated for each voxel within a tumor. From these feature maps we can recognize a number of characteristics like rim enhancement, later wash-out, and heterogeneous or homogeneous enhancement. Those feature maps are described below (formulas are applied for each voxel):

1. Temporal enhancement  $TE_t$  for each time scan:

$$TE_t = \frac{SI_t - SI_0}{SI_0}, \quad 0 \leq t \leq M \tag{1}$$

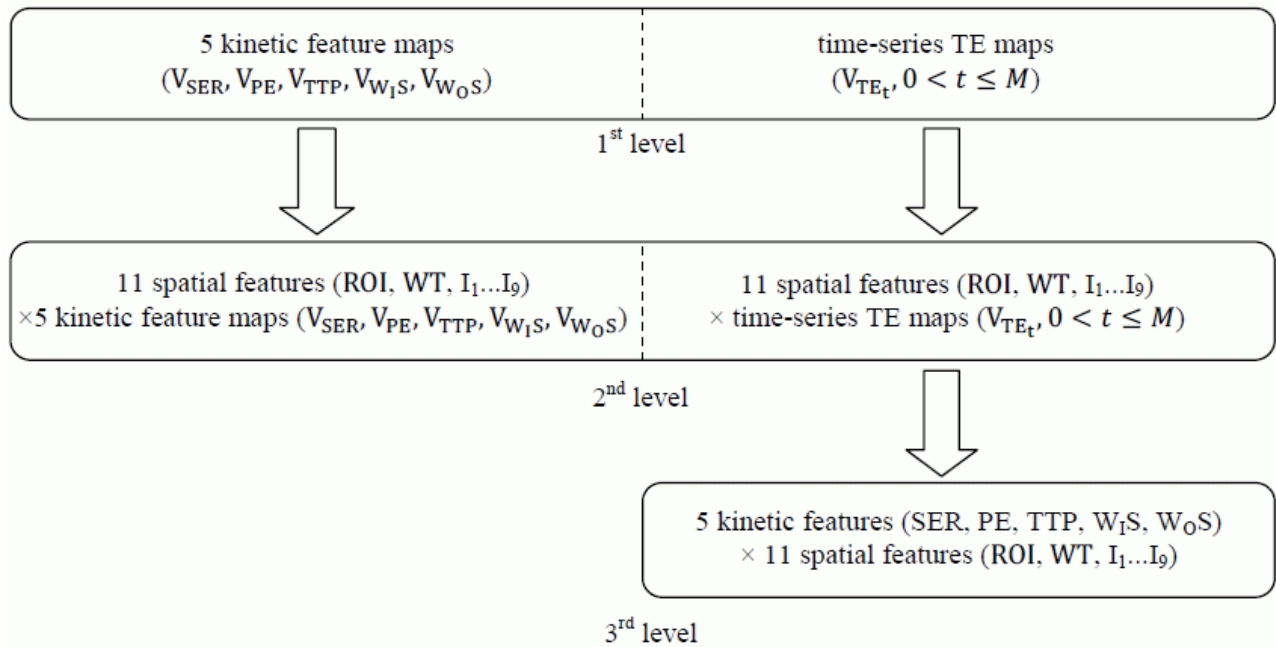


Figure 3. Multilevel feature extraction of spatio-temporal information.

where  $SI_t$  is the post-contrast signal intensity at time frame  $t$  and  $SI_0$  is the pre-contrast signal intensity.  $M$  represents the total number of time scans and equals 5.

2. Peak enhancement  $PE$  is defined as  $\max_{0 \leq t \leq M} TE_t$  and represents the maximum enhancement at a given time scan.
3. Time to peak  $TTP$  is the time at which  $PE$  occurs.
4. Wash-in slope  $WIS$  is determined as:

$$WIS = \frac{PE}{TTP} \quad (2)$$

5. Wash-out slope  $WOS$  is determined as:

$$WOS = \begin{cases} \frac{PE - TE_M}{M - TTP} & TTP \neq M \\ 0 & TTP = M \end{cases} \quad (3)$$

where  $TE_M$  denotes the temporal enhancement at the late post-contrast phase.

6. Three-time-point (3TP)-parameters first post-contrast  $S_1$ , last post contrast  $S_2$  and signal enhancement ratio  $SER$ :

$$SER = \frac{S_1}{S_2} \quad (4)$$

For our data, we chose  $S_1$  which is taken at 1.4 min and  $S_2$  at 5.6 min.

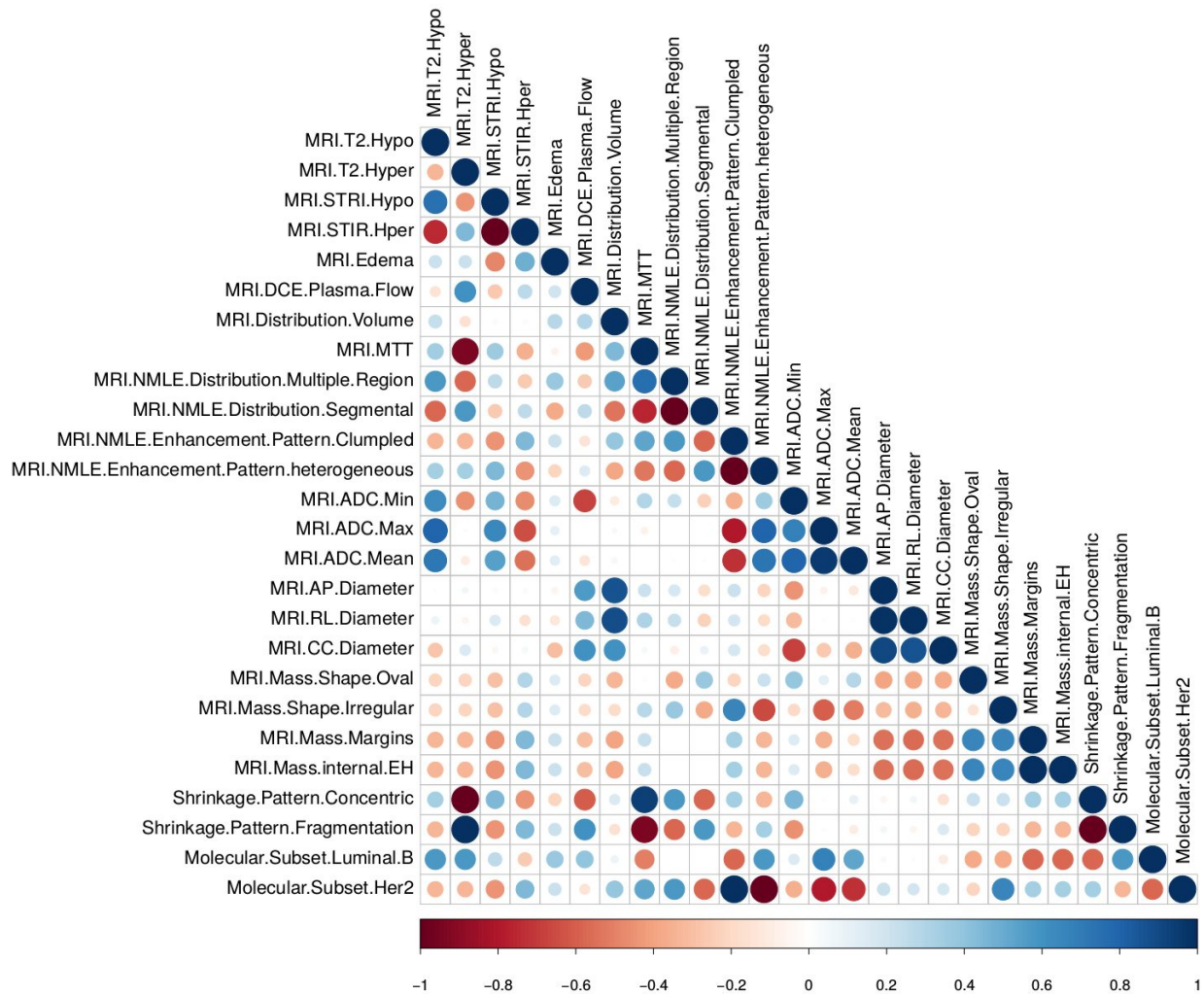


Figure 4. Correlation plot illustration of radiomics features extracted from scan at baseline.

Next we build volumetric images for each voxel for  $S_1$ ,  $S_2$ ,  $SER$ ,  $PE$ ,  $TTP$ ,  $WIS$  and  $WOS$  for representative malignant and benign non-mass-enhancing lesions. Figure 2 shows these maps for typical lesions.

At the second level, eleven spatial features are computed for each of the nine volumetric images of the voxel-wise kinetic features produced at the previous level: mean value of the most enhancing ROI (also called hot spot). At the third level, the five kinetic features  $SER$ ,  $PE$ ,  $TTP$ ,  $WIS$ , and  $WOS$  are additionally computed for the time-series of eleven spatial features computed in the previous step. These features are expected to contain additional information on kinetic association of spatial features within a tumor, which is not available in spatial features computed for the voxel-wise kinetic feature maps. Ninety nine features were obtained for the second level and 55 for the third level. The summary of the feature extraction method based on the multi-level analysis of spatio-temporal information<sup>22</sup> is shown in Figure 3. Moreover, Figure 4 depicts the correlation plot of radiomics features which are extracted from scan at baseline. Blue color present the linear correlation (+1), and the red color presents the inversely-linear correlation (-1), and the size of the circles illustrates the correlation magnitude.

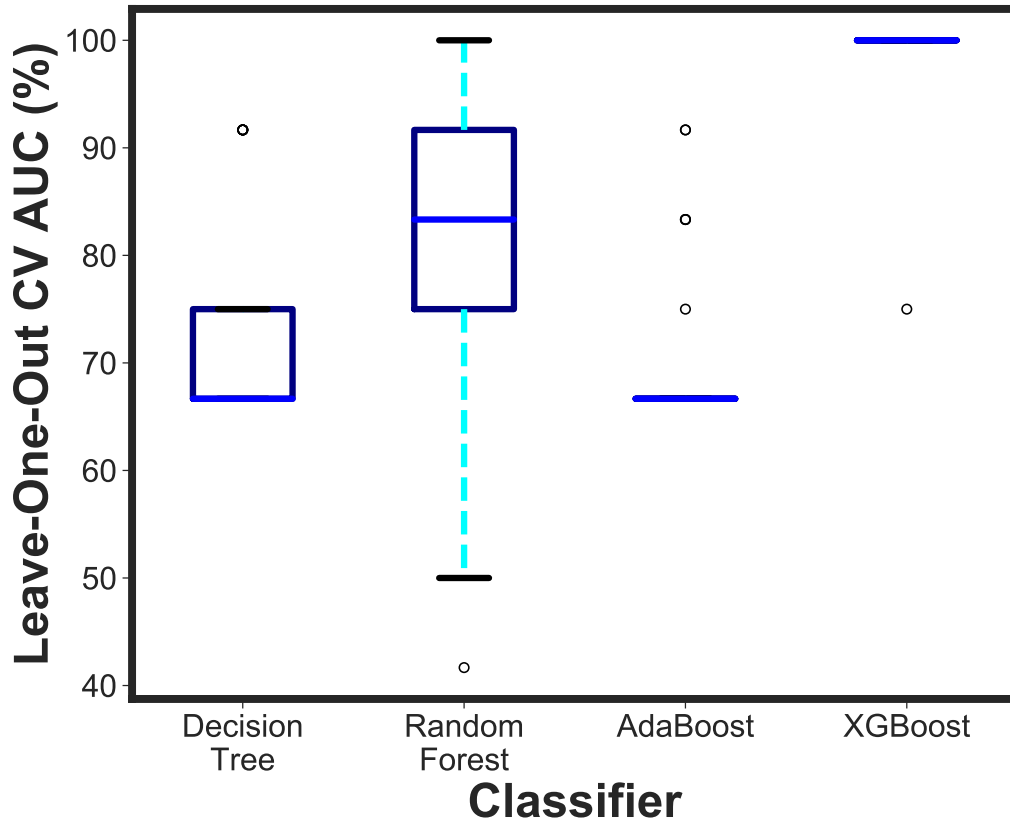


Figure 5. Box plot presentation of AUC score employing leave-one-out cross-validation using classifiers decision tree, random forest, AdaBoost, and XGBoost in early prediction of metastases and death using baseline scans of NAC for four patients.

#### 4. CLASSIFICATION TECHNIQUES AND RESULTS

The following section gives a description of classification methods applied to evaluate the effect of automated classification of diagnostically challenging breast MRI lesions such as foci and non-mass-enhancing lesions based on several feature extraction methods.

Let us assume that  $\mathbf{x}$  describes a  $K$ -dimensional feature vector, that there are  $J$  classes and there are  $N_j$  samples available in group  $j$ . The mean in group  $j$  is given by  $\mu_j$  and the covariance matrix is given by  $\Sigma_j$ .

The classification techniques we employed are support vector machines (SVM) with different kernels, multi-layer perceptrons, and linear logistic regression. SVMs represent an important technique for lesion classification in medical imaging. The key point of this technique is to determine a hyperplane  $H = a\mathbf{v} + b$  that separates the feature vectors  $\vec{v}_i, i = 1, \dots, n$  in their  $d$  dimensional domain in two classes  $\vec{v}_i \in \{M, B\}$ . First, let's assume that our data set is linearly separable and that we can find a pair  $(\vec{w}, b)$  that fulfills:

$$\text{Hyperplanes} = \begin{cases} \vec{w}^T \vec{v}_i + b \geq +1 & \vec{v}_i \in M \\ \vec{w}^T \vec{v}_i + b \leq -1 & \vec{v}_i \in B \end{cases} \quad (5)$$

Furthermore, we want both inequalities to be sharp. The best hyperplane is the one that maximizes the distance (margin) of the two parallel hyperplanes defined in Equation 4. Since the distance of a hyperplane to the origin is  $\frac{b}{\|\vec{w}\|}$  we want to maximize  $\frac{2}{\|\vec{w}\|}$ . This leads to the following constrained optimization problem: Find  $(\vec{w}, b)$  so that  $L(\vec{w}) = \frac{\|\vec{w}\|}{2}$  is minimal subject to the condition:

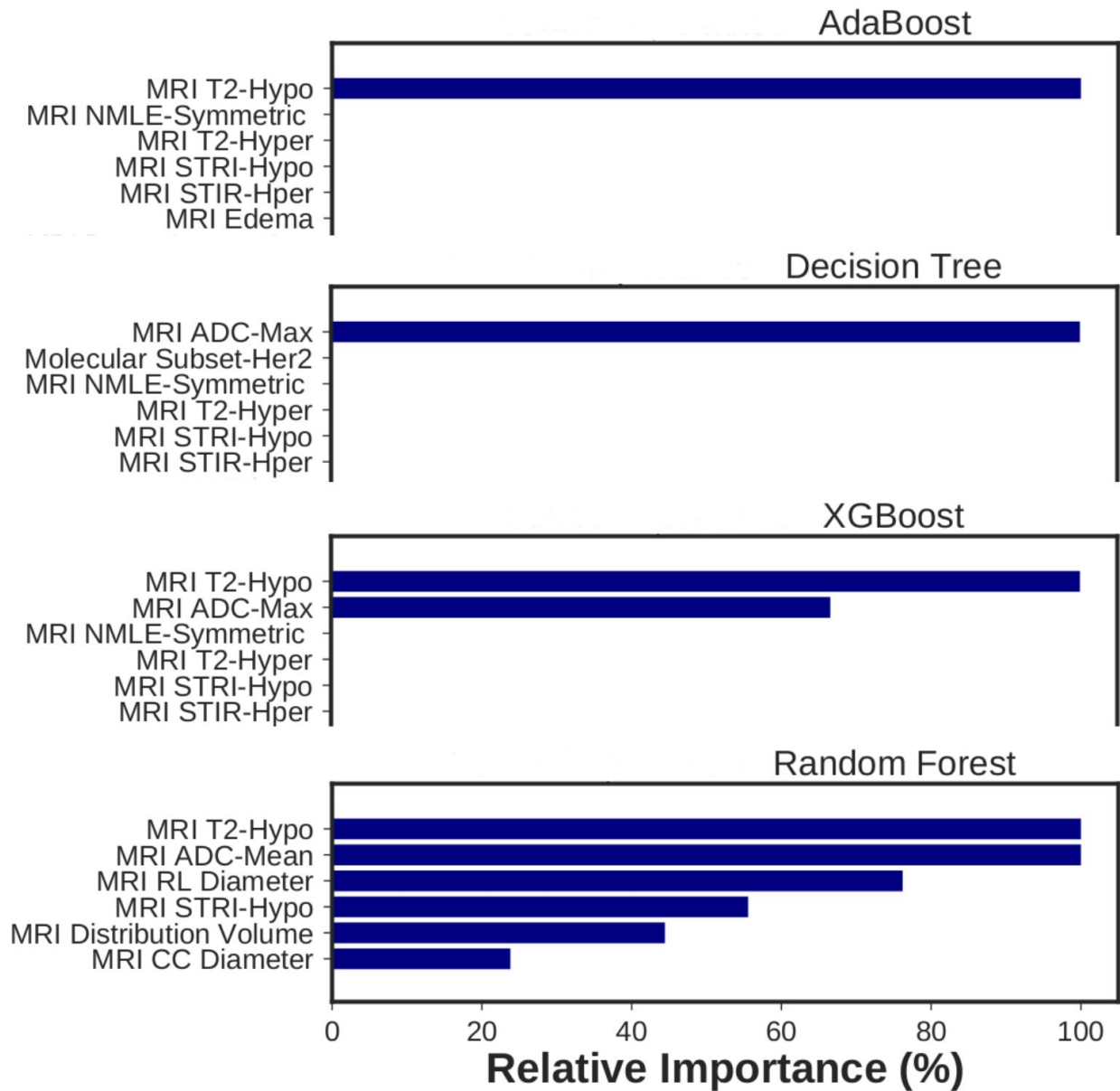


Figure 6. Features importance of classifiers decision tree, random forest, AdaBoost, and XGBoost employing five estimators in early prediction of metastases and death using baseline scans of NAC for four patients.

$$f(\vec{v}_i) = \begin{cases} 1 & \vec{v}_i \in M \\ -1 & \vec{v}_i \in B \end{cases} \quad (6)$$

Of course this only works if all the variables are linearly separable, which cannot be assumed. This problem is solved by introducing positive slack variables  $\theta_i, i = 1, \dots, n$  which leads us to a minimization of  $L(\vec{w}) = \frac{\vec{w}}{2} + \alpha \sum_{i=1}^n \theta_i$  subject to:

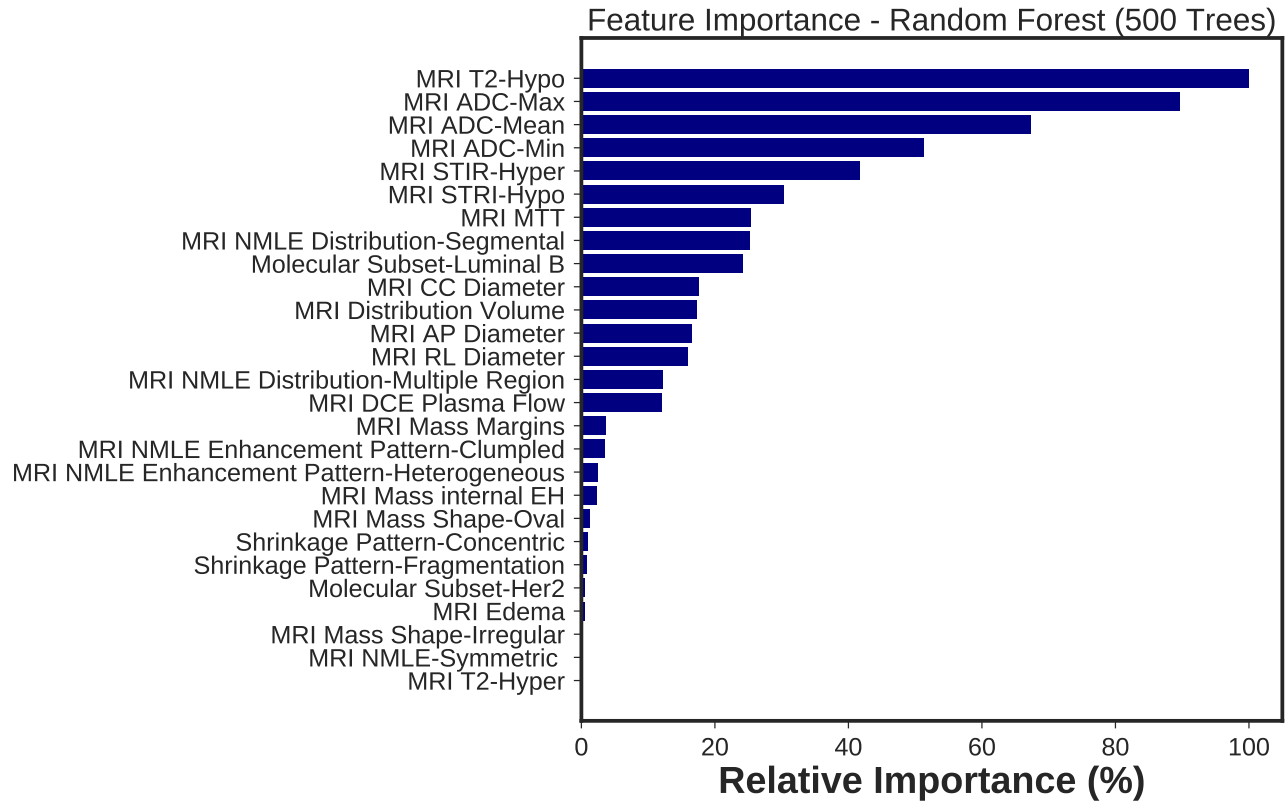


Figure 7. Features importance of random forest classifier using 500 trees in the early prediction of metastases and death using baseline scans of NAC for four patients.

$$f(\vec{v}_i) = \begin{cases} 1 & \text{if } \vec{w}^T \vec{v}_i + b > 1 - \theta_i \\ -1 & \text{if } \vec{w}^T \vec{v}_i + b < -1 + \theta_i \end{cases} \quad (7)$$

An additional challenge appears if there is a non-linear function that separates the variable, since the common approach would fail under these circumstances. Aizerman et al.<sup>23</sup> refined this method by using non-linear kernel functions instead of the scalar product which maps the variables onto another space. The optimal hyperplane computed corresponds to a non-linear function in the original feature space. The polynomial kernel proved to be the optimal kernel in conjunction with the SVM. The area under the curve (AUC) for the 99 second level features was 0.69 and 0.72 for the 55 third-level features. Further we evaluated the systems performance when applying the combined set of all features and applied a number of feature selection algorithms on the set of all available features to select most discriminative features. The best results were obtained when applying Information Gain attribute selection. The best run was obtained with SVM using a polynomial kernel with 70 selected features. The estimated ROC curve of this case with AUC = 0.75.

Additionally, to predict the early response using the NAC data, four classifiers including decision tree, random forest, AdaBoost, and XGBoost were employed.<sup>24-26</sup>

Random forest as an ensemble method employs multiple decision tree classifiers to predict based on the random vectors based on the input data. This randomness should come from a fixed probability distribution. This could be done using bagging which uses uniform probability distribution along with bootstrapped samples of the input dataset. Changing the distribution of the input dataset adaptively through iterations is the essential idea behind the boosting algorithm. Unlike random forest, AdaBoost as one of the famous boosting algorithms, employs different probability distribution to increase the accuracy in prediction of instances which are hard to

Table 1. Classification accuracy of response to early prediction using the NAC data at baseline.

Classifier	AUC $\pm$ STD.
Decision Tree	72.84 $\pm$ 0.14
AdaBoost	70.68 $\pm$ 0.11
Random Forest	82.41 $\pm$ 0.18
XGBoost	<b>99.08 <math>\pm</math> 0.04</b>

classify. Unlike bagging, AdaBoost assigns a weight to each input instance which might change adaptively at the end of each boosting round. Additionally, Gradient tree boosting is also known as gradient boosting machine (GBM) or gradient boosted regression tree (GBRT) is one of the famous method that can be employed to make robust models. In this regard, XGBoost was used as a scalable machine learning system for tree boosting.<sup>24-28</sup>

Figure 5 illustrates the classification accuracy with AUC metric using leave-one-out cross-validation using the NAC data at baseline employing the aforementioned classifiers using five estimators to over-come over-fitting. As shown in Figure 5 and Table 1, XGBoost outperformed the other classification methods dramatically. Additionally, Figure 6 shows the importance of the features participated in the training model for different classifiers with five estimators. As shown, none of the NME features were used in the trained models using five estimators. This could be due to the low number of subjects employed for classification or the lower importance of the NME features at the first sought. However, by training another model for one of the classifiers, i.e. random forest with 500 estimators we can see how important the NME features are in early prediction of response to neo-adjuvant chemotherapy. As shown in Figure 7, NME distributions including segmental and multiple region sub-types are as important as kinetic features and apparent diffusion coefficients. Furthermore, NME enhancement pattern with clumped and heterogeneous sub-types were shown as important as morphological features such mass shapes and the shrinkage pattern of the tumors.

## 5. CONCLUSIONS

NME lesions represent a diagnostically challenging type of breast tumors, are easily missed by radiologists, and therefore require a careful reading. An automated procedure would be highly desirable, however, neither typical kinetic nor morphologic parameters distinctive for these lesions are so far known. A fusion of multi-level features proved to be the key descriptors for detection and classification of NMEs in an automated CAD system. Additionally, the NME features show a reasonable importance in early prediction of response to neo-adjuvant chemotherapy using robust models.

## 6. ACKNOWLEDGEMENTS

This research was supported in part by NIH Grant 5K25CA106799-05. The authors also would like to thank Tessa Daniels for the careful revision of the manuscript.

## Appendix: List of Abbreviations

- NMLE: Non-Mass-Like-Enhancing
- NME: Non-Mass-Enhancing
- CAD: Computer Aided Diagnosis
- DCE-MRI: Dynamic Contrast-Enhanced Magnetic Resonance Imaging
- NAC: Neo-Adjuvant Chemotherapy
- pCR: Pathological Complete Response
- STIR: Short TI Inversion Recovery
- DWI: Diffusion Weighted Imaging
- ROI: Region Of Interest
- ICA: Independent Component Analysis
- $TE$ : Temporal Enhancement
- $SI_t$ : Post-Contrast Signal Intensity at Time Frame  $t$
- $SI_0$ : Pre-Contrast Signal Intensity
- $PE$ : Peak Enhancement
- $TE_t$ : Maximum Enhancement at Time Frame  $t$
- $TTP$ : Time To Pick
- $WIS$ : Wash-In Slope
- $WOS$ : Wash-Out Slope
- $TE_M$ : Temporal Enhancement at the Late Post-Contrast Phase
- $S_1$ : First Post-Contrast Signal
- $S_2$ : Last Post-Contrast Signal
- $SER$ : Signal Enhancement Ratio
- ROC: Receiver Operating Characteristic
- AUC: Area Under Curve
- SVM: Support Vector Machine
- CV: Cross-Validation
- GBRT: Gradient Boosted Regression Tree
- GBM: Gradient Boosting Machine

## REFERENCES

- [1] Vag, T., Baltzer, P., Dietzel, M., Zoubi, R., Gajda, M., Camara, O., and Kaiser, W., “Intravoxel incoherent motion (ivim) in evaluation of breast lesions: Comparison with conventional dwi,” *European Journal of Radiology* **21**, 782–789 (2 2013).
- [2] Yabuuchi, H., Matsuo, Y., Kamitani, T., Setoguchi, T., Okafuji, T., Soeda, H., Sakai, S., Hatekenata, M., Kubo, M., Tokunaga, E., Yamamoto, H., and Honda, H., “Non-mass-like enhancement on contrast-enhanced breast mri imaging: Lesion characterization using combination of dynamic contrast-enhanced and diffusion-weighted mr images,” *European Journal of Radiology* **75**, 126–132 (2 2010).
- [3] Retter, F., Plant, C., Burgeth, B., Schlossbauer, T., and Meyer-Baese, A., “Improved computer-aided diagnosis for breast lesions detection in dce-mri based on image registration and integration of morphologic and dynamic characteristics,” *SPIE Symposium Computational Intelligence* **8059**, 8059OJ (7 2011).
- [4] Hoffmann, S., Burgeth, B., Lobbes, M., and Meyer-Baese, A., “Automatic evaluation of single and joint kinetic and morphologic features for non-masses,” *SPIE Symposium Computational Intelligence* **8401**, 8401–38 (7 2012).
- [5] Hoffmann, S., Burgeth, B., Lobbes, M., and Meyer-Baese, A., “How effective is kinetic, morphologic, and mixed analysis for both mass and non-mass lesions?,” *SPIE Symposium Computational Intelligence* **8401**, 8401–39 (7 2012).
- [6] Zheng, Y., Englander, S., Baloch, S., Zacharaki, E., Fan, Y., Schnall, M., and Shen, D., “Step: Spatiotemporal enhancement pattern for mr-based breast tumor diagnosis,” *Medical Physics* **36**, 3192–3204 (7 2009).
- [7] Retter, F., Plant, C., Burgeth, B., Botilla, G., Schlossbauer, T., and Meyer-Baese, A., “Computer-aided diagnosis for diagnostically challenging breast lesions in dce-mri based on image registration and integration of morphologic and dynamic characteristics,” *EURASIP Journal on Advances in Signal Processing*, 2013:157 (4 2013).
- [8] Hoffmann, S., Shutler, J. D., Lobbes, M., Burgeth, B., and Meyer-Baese, A., “Automated analysis of diagnostically challenging lesions in breast mri based on spatio-temporal moments and joint segmentation-motion compensation technique,” *EURASIP Journal on Advances in Signal Processing*, 2013:172 (4 2013).
- [9] Newell, D., Nie, K., Chen, J., Hsu, C., Yu, H., Nalcioglu, O., and Su, M., “Selection of diagnostic features on breast mri to differentiate between malignant and benign lesions using computer-aided diagnostics: Differences in lesions presenting as mass and non-mass-like enhancement,” *European Radiology* **20**, 771–781 (2 2010).
- [10] Tahmassebi, A., Pinker-Domenig, K., Wengert, G., Helbich, T., Bago-Horvath, Z., and Meyer-Baese, A., “Determining the importance of parameters extracted from multi-parametric mri in the early prediction of the response to neo-adjuvant chemotherapy in breast cancer,” in [*Medical Imaging 2018: Biomedical Applications in Molecular, Structural, and Functional Imaging*], **10578**, International Society for Optics and Photonics (2018).
- [11] Tahmassebi, A., Meyer-Baese, A., Wengert, G., Helbich, T., and Pinker-Domenig, K., “Radiomics with mri for early prediction of the response to neo-adjuvant chemotherapy in breast cancer patients,” in [*Insights into Imaging*], Springer (2018).
- [12] Pinker-Domenig, K., Tahmassebi, A., Wengert, G., Helbich, T., Bago-Horvath, Z., Morris, E. A., and Meyer-Baese, A., “Magnetic resonance imaging of the breast and radiomics analysis for an improved early prediction of the response to neoadjuvant chemotherapy in breast cancer patients,” in [*In: Proceedings of the 109th Annual Meeting of the American Association for Cancer Research*], **579/22**, AACR (2018).
- [13] Chan, T. and Vese, L., “Active contours without edges,” *IEEE Transactions on Image Processing* **10**, 266–277 (9 2001).
- [14] Theis, F. J., Meyer-Baese, A., and Lang, E., “Second-order blind source separation based on multi-dimensional autocovariances,” *Lecture Notes in Computer Science, Vol. 3195*, 726–733 (9 2004).
- [15] Theis, F., Gruber, P., Keck, I., Meyer-Bäse, A., and Lang, E., “Spatiotemporal blind source separation using double-sided approximate joint diagonalization,” *Proc. EUSIPCO 2005* (2005).
- [16] Meyer-Baese, A., Gruber, P., Thies, F., and Foo, S., “Blind source separation based on self-organizing neural network,” *Engineering Applications of Artificial Intelligence*, 305–311 (4 2006).

- [17] Meyer-Bäse, A., Watzel, R., Meyer-Bäse, U., and Foo, S., “A parallel cordic architecture to compute the gaussian potential function in neural networks,” *Engineering Application of Artificial Intelligence*, 595–605 (9 2003).
- [18] Meyer-Bäse, U., Vera, A., Meyer-Bäse, A., Pattichis, M., and Perry, R., “Discrete wavelet-transform fpga using matlab/simulink,” *SPIE’s 20th Annual International Symposium on Aerospace/ Defense Sensing, Simulation and Controls, Vol. 6247*, 624703 (9 2006).
- [19] Meyer-Bäse, U., Meyer-Bäse, A., Mellott, J., and Taylor, F., “A fast modified CORDIC-implementation of radial basis neural networks,” *Journal of VLSI SIGNAL PROCESSING SYSTEMS for Signal, Image and Video Technology* **9**, 290–298 (1998).
- [20] Meyer-Bäse, U. and Meyer-Bäse, A., “Coordinate rotation digital computer (cordic) synthesis for fpga,” *Lecture Notes in Computer Science 849, Springer Verlag*, 397–409 (9 1994).
- [21] Meyer-Bäse, A., Meyer-Bäse, U., Mellott, J., and Taylor, F., “A fast modified cordic-implementation of radial basis neural networks,” *Journal of VLSI SIGNAL PROCESSING SYSTEMS for Signal, Image, and Video Technology*, 290–298 (9 1998).
- [22] Lee, S., Kim, J., Yang, Z., Jung, Y., and Moon, W., “Multilevel analysis of spatiotemporal association features for differentiation of tumor enhancement pattern in breast dce-mri,” *Medical Physics* **37**, 3940–3956 (7 2010).
- [23] Aizerman, M., Braverman, E., and Rozonoer, L., “Theoretical foundations of the potential function method in pattern recognition learning,” *Automation and Remote Control*, 821837 (25 1964).
- [24] Duda, R. O., Hart, P. E., and Stork, D. G., [*Pattern classification*], John Wiley & Sons (2012).
- [25] Pedregosa, F., Varoquaux, G., Gramfort, A., Michel, V., Thirion, B., Grisel, O., Blondel, M., Prettenhofer, P., Weiss, R., Dubourg, V., et al., “Scikit-learn: Machine learning in python,” *Journal of machine learning research* **12**(Oct), 2825–2830 (2011).
- [26] Chen, T. and Guestrin, C., “Xgboost: A scalable tree boosting system,” in [*Proceedings of the 22nd acm sigkdd international conference on knowledge discovery and data mining*], 785–794, ACM (2016).
- [27] Illan, I. A., Tahmassebi, A., Ramirez, J., Gorriz, J. M., Foo, S. Y., Pinker-Domenig, K., and Meyer-Bäse, A., “Machine learning for accurate differentiation of benign and malignant breast tumors presenting as non-mass enhancement,” in [*Computational Imaging III*], **10669**, International Society for Optics and Photonics (2018).
- [28] Tahmassebi, A., “ideeple: Deep learning in a flash,” in [*Disruptive Technologies in Information Sciences*], **10652**, International Society for Optics and Photonics (2018).